Stanford Exploration Project, Report 115, May 22, 2004, pages 191–199

Residual move-out analysis with 3-D angle-domain common-image gathers

Thomas Tisserant and Biondo Biondi[1]

ABSTRACT

We describe a method to update the velocity model from the residual move-out information contained in 3-D angle-domain common-image gathers. The 3-D angle-domain common-image gathers computed after wave-equation migration are functions of the aperture angle and the reflection azimuth angle. We perform a velocity error analysis by semblance using 2-D and 3-D residual move-out functions. Both functions enable us to update the velocity model. The 3-D function leads to a better estimation of the velocity error in the case of 3-D events.

INTRODUCTION

Migration velocity analysis combines migration and velocity analysis in an iterative process. After each migration, if the velocity model is not correct, the events in the common-image gathers (CIGs) are not flat. Migration velocity analysis uses the residual move-out (RMO) in the gathers to update the velocity model.

Wavefield-continuation migration offset-domain common-image gathers (ODCIGs) generated are inconvenient for extracting velocity information. Conversely, wavefield-continuation migration angle-domain common-image gathers (ADCIGS) are convenient because their energy is spread over the gather, similar to ODCIGs in Kirchhoff migration. In addition, ADCIGs avoid ambiguities of the reflector positions in Kirchhoff ODCIGs when multipathing occurs (Prucha et al., 1999).

The ADCIGs can be formed during the imaging step of the wavefield-continuation migration (de Bruin et al., 1990; Prucha et al., 1999). In this case, the ADCIGs are expressed in terms of the offset ray-parameter instead of the aperture angle. Sava and Fomel (2003) propose a method applied after imaging to obtain ADCIGs as functions of the direct aperture angle. Pointing out that the method is valid only for reflectors orthogonal to the acquisition direction (dip-reflection), and consequently ignores the azimuth angle of the reflection, Biondi and Tisserant (2004) generalize it to 3-D. The resulting ADCIGs are not only function of aperture angle, but also function of reflection azimuth angle.

As well as providing additional information to perform velocity analysis, the knowledge of

[1]**email:** thomas@sep.stanford.edu, biondo@sep.stanford.edu

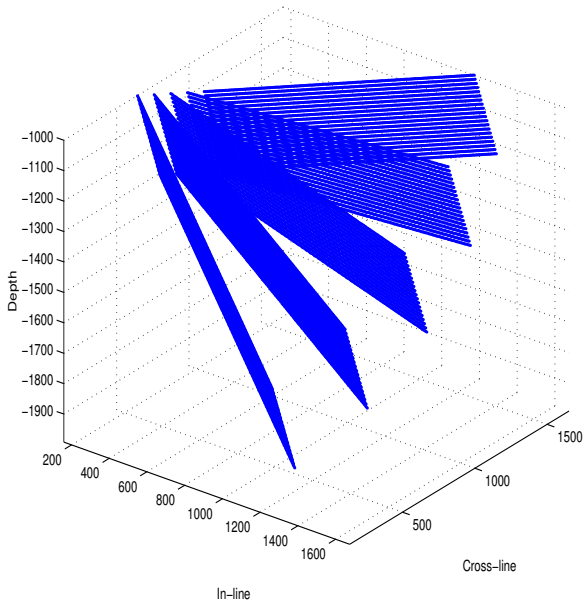

Figure 1: 5 reflectors with an azimuth of 45° and dips from 0° to 60°. The velocity function is $v = 1500 + 0.5\ z$ m/s. thomas1-planes [NR]

the reflection azimuth can also be used to correctly backproject rays in reflection tomography, or to perform amplitude-versus-angle analysis along the reflection azimuth at the image point rather than along the acquisition azimuth.

Biondi and Symes (2003) analyze the kinematics of the ADCIGs in the presence of velocity error and derive an RMO function. Biondi and Tisserant (2004) extend this study to 3-D. This paper describes the estimation of the velocity error from 3-D ADCGIs in order to update the velocity model. We first review the additional information contained by the 3-D ADCIGs. We then quantify the velocity error from the ADCIGs with a 2-D RMO function. The last part describes how accounting for the 3-D wave propagation improves the estimation of the velocity error. The method is tested on the synthetic model displayed in Figure 1. The model consists of 5 dipping planes in a linearly increasing velocity $v(z) = 1500 + .5z\ m.s^{-1}$. The planes have a 45° azimuth. The dataset is migrated with a full prestack wavefield-continuation migration and a velocity that is 3% too low.

3-D ANGLE-DOMAIN COMMON-IMAGE GATHERS

Our velocity-error estimation method uses ADCIGs computed after imaging through an offset-to-angle transformation (Sava and Fomel, 2003). Although valid in 2-D, Biondi et al. (2003) point out that the transformation assumes the azimuth of the reflectors to be orthogonal to the azimuth of the acquisition (dip-reflections). The transformation also ignores the reflection azimuth. The reflection azimuth is equal to the acquisition azimuth when the rays do not bend (in constant velocity), or in case of dip-reflections. Biondi and Tisserant (2004) extend the method to 3-D. The transformation maps the migrated inline and cross-line offsets into the aperture angle (γ) and reflection azimuth angle (ϕ). Hence, after being transformed to the angle domain, each CIG is a (z,γ,ϕ) cube.

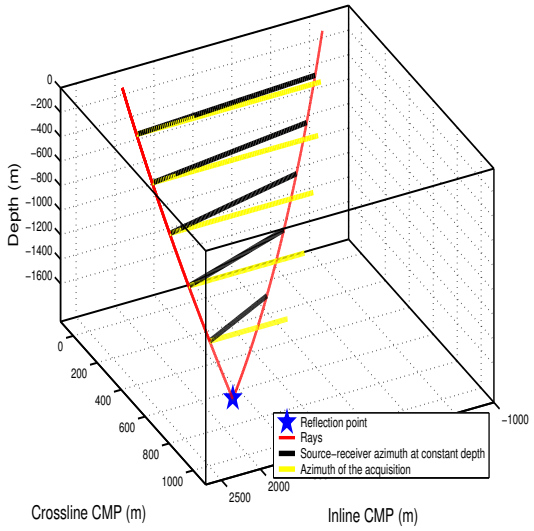

Figure 2: Source and receiver rays for one event on a 45° dip reflector with a 45° azimuth. thomas1-rays [CR]

following the characteristics of the fourth reflectors on the model displayed in Figure 1, Figure 2 simulates a reflection from a reflector with a 45° dip and a 45° azimuth in a vertically increasing velocity. It illustrates how different the reflection azimuth can be from the acquisition azimuth in a 3-D configuration. The gray lines symbolize the survey azimuth at constant depth. The black lines symbolize the azimuth between the source and receiver rays at each depth. At the reflection position, the angle between the black and green lines is the reflection azimuth.

Figure 3 shows slices of the (z,γ,ϕ) cube at constant ϕ for two CIGs from the model. The top row is the CIG taken at x=700m and y=700m, where the steepest reflector is not visible. The bottom row is the CIG taken at x=425m and y=425m, where only the two steepest reflectors are visible. For the remainder of this paper, we will refer to these two CIGs as CIG_{700} and CIG_{425}. On both rows, the first panel is the stack over the ϕ dimension of the cube. The other panels are slices of the cube at constant ϕ. As ϕ increases, the gathers frown downward, then smile upward, reach a maximum, and frown down again. Note that, although the velocity is incorrect, the gathers are flat for some values of ϕ. Each event is stationary at one particular value of ϕ when the smile is at its maximum. For CIG_{700}, ϕ is around 0° for 0° dip and 15° dip reflectors, around 3° for the 30° dip reflector, and a bit higher than 6° for the 45° dip reflector. For CIG_{425}, ϕ is around 5° for 45° dip, and around 16° for the 60° dip reflector. Notice that the values of ϕ from one CIG to another are comparable for reflectors with the same dip. Since the gathers are stationary for the correct ϕ value, the stack carries some information about the reflection azimuth.

This analysis can be done whether the migration velocity is correct or not. If the velocity is incorrect, however, the measured values are apparent reflection azimuth angles. The difference between the true reflection azimuth and the apparent one is due to the incorrect ray-bending when the velocity is incorrect.

We next describe how to estimate the velocity error from the ADCIGs with a RMO function.

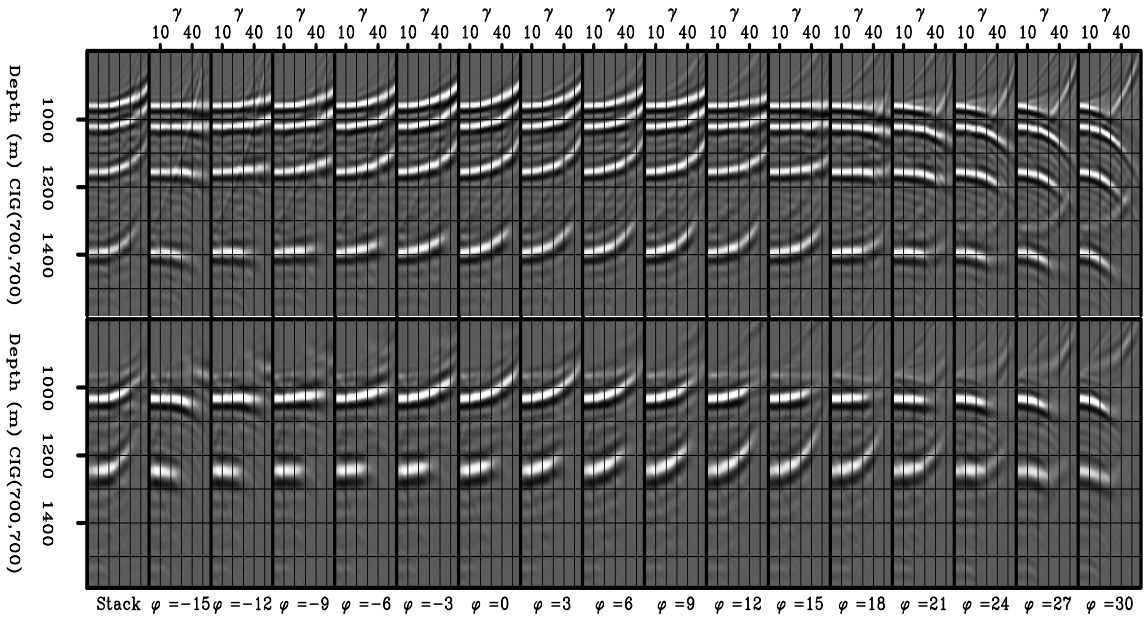

Figure 3: Behavior of two CIGs with the reflection azimuth ϕ. On the top row: CIG_{700}. The visible reflectors are dipping 0°, 15°, 30°, and 45°. On the bottom row: CIG_{425}. The visible reflectors are dipping 45° and 60°. For both CIGs, the first two panels on the left are stacks over ϕ. The other panels are slices of the cube (z,γ,ϕ) at constant ϕ. thomas1-find_phi [ER]

ESTIMATING THE VELOCITY ERROR WITH A 2-D RMO FUNCTION

Migrating with an incorrect velocity results in gathers frowning downward if the velocity is too high, and gathers smiling upward if the velocity is too slow. Biondi et al. (2003) analyze the kinematics of ADCIGs. Assuming stationary-raypath, or straight rays, the authors show that the apparent image point in the angle domain is located on the normal to the apparent reflector, and provide a 2-D RMO function to quantify the amount of the shift of the image point:

$$\Delta n_{RMO} = \frac{1-\rho}{\cos\alpha}\frac{\sin^2\gamma}{(\cos^2\alpha - \sin^2\gamma)} z_0, \tag{1}$$

where ρ is the ratio between the slowness used for the migration and the true slowness, *i.e.*, a measure of the velocity error, α the dip of the reflector, γ the aperture angle, and z_0 the depth of the reflector. In the case of a flat reflector ($\alpha = 0$), equation (1) reduces to

$$\Delta n_{RMO} = (\rho - 1)\tan^2\gamma \; z_0. \tag{2}$$

The parameter we want to estimate is ρ. The RMO is measured along the normal to the reflector but can be applied along the vertical after scaling with the cosine of the dip.

Both functions are tested on two CIGs of the model displayed in Figure 1. Figure 4 illustrates a velocity error analysis by semblance. The top row is CIG_{700}, and the bottom row

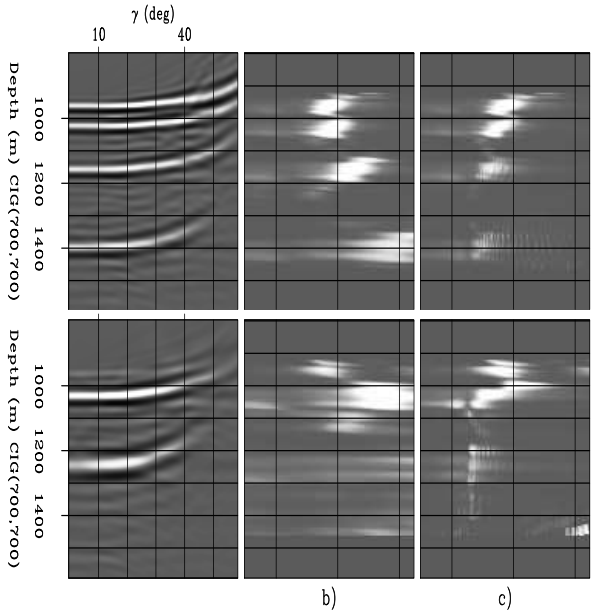

Figure 4: Velocity error analysis by semblance using a 2-D RMO function on CIG_{700} on the top row, and on CIG_{425} on the bottom row. a) Stack over ϕ of CIG (425,425). b) Semblance analysis of the first panel with a zero-dip assumption. c) Semblance analysis of the first panel with the dip information. Both semblance panels are squared to increase resolution. thomas1-stk_2D_700_450 [ER]

is CIG_{425}. The dips for CIG_{700} range from 0° to 45°. The dips for CIG_{700} range from 45° to 60°. Figure 4a is the stack over ϕ for the two CIGs. The upward smiles indicate that the migration velocity is too low. The velocity error being 3%, the peak of semblance will ideally be centered at $\rho = 1.03$.

Figure 4b is the velocity error spectrum of the left panels in the absence of dip information and using $\alpha = 0$ (equation (2)). As expected, the peak of semblance is correctly positioned for the flat reflector at depth 960 m. However, the other peaks of semblance are mispositioned for the steeper reflectors, where the zero-dip assumption is not valid. For the steepest reflector, the peak of semblance is out of the semblance panel.

Figure 4c is the velocity error spectrum of the left panel, using the RMO function with the knowledge of the dip (equation (1)). The dip does not have to be known *a priori*; it can be extracted from the migrated cube between the migration step and the velocity error estimation step. The peaks of semblance are better focused but are still not accurate enough, especially for the steepest reflector, on which we read $\rho = 1$, signifying that the velocity is correct. To correct this, we need to take into account 3-D events.

The 2-D RMO functions can be used to extract the velocity error from the gathers of the migrated cube. The simple RMO function works for flat reflectors. When the dip information in included, the RMO function corrects the error generated by steeply dipping reflectors. However, the peaks are not correctly positioned because of 3-D events that are not appropriately processed by equation (1).

IMPROVING THE ESTIMATION WITH A 3-D RMO FUNCTION

Biondi and Tisserant (2004) extend the 2-D RMO function (equation (1)) to a 3-D function

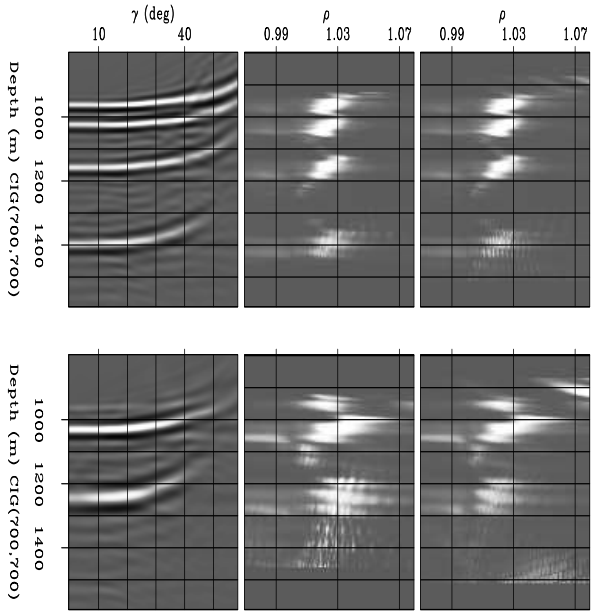

Figure 5: Velocity error analysis by semblance using a 3-D RMO function on CIG_{700} on the top row, and on CIG_{425} on the bottom row. a) CIG after stack over ϕ. b) Semblance analysis of the left panel using the 3-D RMO function at $\phi = 0$. c) ϕ semblance analysis. d) Semblance analysis of the first panel using the 3-D RMO function with a $\phi(z)$ law. All semblance panels are squared to increase resolution. thomas1-stk_3D_700_450 [ER]

that includes the azimuth of the reflector (η), and the azimuth of the reflection (ϕ):

$$\Delta n_{RMO} = \frac{\rho - 1}{\cos\alpha} \frac{\sin^2\gamma\sqrt{1-\sin^2\alpha\cos^2(\eta-\phi)}}{\left(1-\sin^2\alpha\cos^2(\eta-\phi)-\sin^2\gamma\right)} z_0. \tag{3}$$

Equation (1) is a special case of equation (3), where the azimuth of the acquisition and the reflection are the same ($\eta = \phi$): the 2-D RMO function implicitly assumes dip-reflections just as the 2-D offset-to-angle transformation does. In the case of a flat reflector ($\alpha = 0$), the RMO functions are the same in 2-D and 3-D, because horizontal planes have no defined azimuth and do not generate 3-D reflection.

Figure 5 synthesizes all the velocity analysis done with equation (3) on two CIGs taken from the model. CIG_{700} (top) and CIG_{425} (bottom) stacked over ϕ are represented in Figure 5a.

Figure 5b is the semblance analysis of the stack using the 3-D RMO function (equation (3)), with $\eta = 45°$ (the true azimuth of the reflectors) and assuming $\phi = 0°$ in the absence of ϕ information. For the first CIG, the comparison with the semblance panel obtained with the 2-D RMO function (Figure 4c) shows a more accurate resolution of the velocity error when the reflector azimuth is provided.

We perform a semblance analysis to determine the reflection azimuth. The procedure consists in scanning all the slices at constant ϕ of the (z,γ,ϕ) cube using equation (3), with the velocity error obtained from a previous analysis performed on the stack with the $\phi = 0$ assumption (Figure 5b). Then, only the trace corresponding to the measured velocity error is taken from each semblance panel at constant ϕ. All the traces displayed side by side form the ϕ semblance panel displayed in Figure 6. The peaks of semblance give the reflection azimuth for each event. The value of ϕ ranges from 0° to 7° for the first CIG, and from 6° to 16° for the second CIG. They are consistent with the ϕ values read on Figure 3. Once again, the reflection

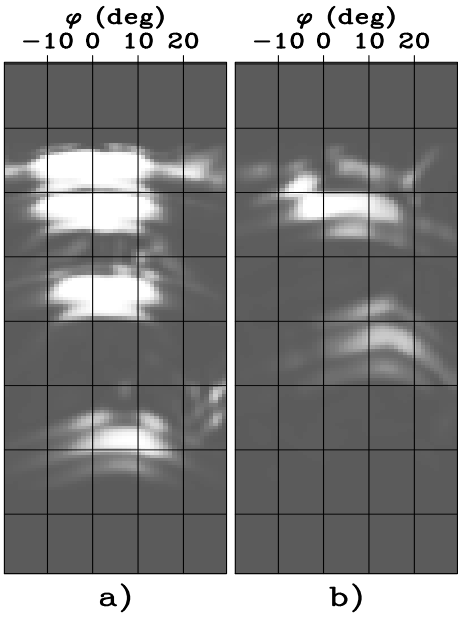

Figure 6: Reflection azimuth analysis using a 3-D RMO function on a) CIG_{700} b) CIG_{425}. All semblance panels are squared to increase resolution. thomas1-pfan_700_450 [ER]

azimuths are comparable at similar reflector dips.

Figure 5c adds the reflection azimuth information picked in Figure 6 to the velocity error analysis. This extra information does not improve the resolution of the velocity error for the first CIG, where the range of ϕ is limited and satisfies the $\phi = 0$ assumption because of the limited dips. Note that the peaks of semblance are not centered perfectly on $\rho = 1.03$ but are closer to $\rho = 1.025$. This underestimated velocity error is due to the straight rays assumption that over-corrects the move-out.

For the second CIG, where the $\phi = 0$ assumption is not valid, we expect some changes. Paradoxically, the estimation seems less accurate for the 60° reflector when the value of ϕ is used ($\rho = 1.02$) instead of setting ϕ to 0 ($\rho = 1.03$). The reason is when the $\phi = 0$ approximation is not valid, the RMO function over-estimates the velocity error. Simultaneously, the RMO function under-estimates the velocity error because of the straight rays approximation. Hence the errors cancel out and make the estimation apparently more accurate with the $\phi = 0$ assumption than with the correct value of ϕ.

The 3-D analysis of the RMO in the ADCIGs improves the resolution of the velocity error, even if the knowledge of the reflection azimuth does not bring visible improvement. The precise estimation of the reflection azimuth still holds for tomographic or amplitude-versus-angle studies.

CONCLUSION

We have presented a method to estimate the error in the migration velocity. It is based on the analysis of the residual move-out in 3-D angle-domain common-image gathers. The 3-D ADCIGs are functions of the aperture angle and the reflection azimuth angle. We tested a 2-D

and a 3-D RMO function that led to an estimation of the velocity error and made it possible to update the velocity model. Because of 3-D events, the 2-D estimation of the velocity error is not accurate enough. The 3-D approach accounted for 3-D events and improved the resolution of the error. All the parameters required to estimate precisely the RMO function (the dips of the reflectors, the azimuth of the reflectors, and, to a minor extent, the reflection azimuth) can be estimated from the migrated data. The method can be automated and can serve as a basis for migration velocity analysis.

REFERENCES

Biondi, B., and Symes, W., 2003, Angle-domain common-image gathers for migration velocity analysis by wavefield-continuation imaging: Geophysics: submitted for publication.

Biondi, B., and Tisserant, T., 2004, Angle-domain common-image gathers for wave-equation velocity analysis: Geophysical Prospecting: submitted for publication.

Biondi, B., Tisserant, T., and Symes, W., 2003, Wavefield-continuation angle-domain common-image gathers for migration velocity analysis: Soc. of Expl. Geophys., 73rd Ann. Internat. Mtg., 2104–2107.

de Bruin, C. G., Wapenaar, C. P. A., and Berkhout, A. J., 1990, Angle-dependent reflectivity by means of prestack migration: Geophysics, **55**, no. 9, 1223–1234.

Prucha, M., Biondi, B., and Symes, W., 1999, Angle-domain common-image gathers by wave-equation migration: Soc. of Expl. Geophys., 69th Ann. Internat. Mtg, 824–827.

Sava, P. C., and Fomel, S., 2003, Angle-domain common-image gathers by wavefield continuation methods: Geophysics, **68**, no. 3, 1065–1074.